

Jules Allbritton-King^{1,2}, Megan Kimicata^{2,3}, John P. Fisher, PhD^{1,2}

¹Fischell Department of Bioengineering, University of Maryland, College Park MD

²Center for Engineering Complex Tissues, University of Maryland, College Park, MD

³Department of Materials Science and Engineering, University of Maryland, College Park, MD

Introduction

Chronic, nonhealing wounds affect about 6.5 million individuals in the U.S., and often present as comorbidities of other prevalent conditions such as obesity and diabetes.¹ Chronic wounds are characterized by a recurring inflammatory state without progression to the proliferation and remodeling stages of wound healing. Around \$25 billion is spent annually on treatment of chronic wounds; however most traditional wound care approaches do not effectively encourage the physiological healing process.² One emerging treatment option is extracellular matrix (ECM)-based wound dressings, which are composed of a network of proteins and other macromolecules that support and anchor cells within tissue. These dressings are typically composed of decellularized tissue derived from animal donors and provide a protein scaffold that mimics dermal ECM by facilitating cell adhesion. Most commercially available ECM-based dressings are dry, uniform sheets of ECM that provide a structural scaffold for cellular growth, but do not provide a physiologically relevant moisture balance or encourage cellular infiltration into the dressing as the wound heals. However, fibroblasts, which play a major role in wound healing, have been shown to migrate to regions of denser ECM concentrations, where they exhibit enhanced metabolic activity and proliferation.³

A UBM-based hydrogel will serve as an alternative wound dressing that will mitigate the issues with current ECM-based products. A hydrogel dressing offers a more physiologically relevant moisture balance to the site of the wound, while integrated structural cues will encourage fibroblast infiltration. Ultimately, this approach will increase the rate at which ulcers heal and prevent further deterioration of the wound site, in turn lessening the physical and financial burden on patients.

Objective

The objective of this work is to design a hydrogel containing a gradient of porcine urinary bladder matrix (UBM) concentrations for wound dressing applications and to characterize its cellular response, rheological properties, and *in vitro* collagenase degradation.

Porcine Urinary Bladder Matrix

Bladder Dissection and UBM Delamination

Whole porcine bladders (Animal Biotech) were distended with 1L of PBS using a syringe and left overnight. The bladders were drained, cut open, and the detrusor muscle layer was mechanically delaminated from the luminal tissue. The resulting biomaterial is known as urinary bladder matrix (UBM).⁴

Decellularization and DNA Quantification

Protocol was adapted from a procedure developed by Gui et. al.⁵ Briefly, LB-ECM was rinsed in a hypotonic PIPES buffer followed by an SDS buffer. Finally, tissue was rinsed in endothelial cell medium. DNA content in UBM before and after decellularization was quantified via PicoGreen assay. Additionally, to qualitatively assess decellularization, native and decellularized UBM samples were fixed in paraformaldehyde, embedded in paraffin, sectioned, and stained with H&E.

UBM-Based Hydrogels

UBM Digestion and Gelation

Decellularized UBM was lyophilized, digested, and reconstituted as a hydrogel as previously described.⁶ Briefly, decellularized UBM was lyophilized overnight, ground into a particulate form, and digested in a pepsin solution. The fully digested UBM solution was then neutralized, diluted, and injected into a cylindrical mold. Thermal gelation occurred when the pre-gel was heated to 37° C.

UBM Gradient Hydrogel Fabrication

Gels with a gradient were fabricated by layering equal volumes of pre-gel solutions containing different UBM concentrations prior to gelation. Pre-gel solutions were viscous enough to prevent mixing, resulting in a three-layered gradient of differing UBM concentrations following gelation.

Decellularization & Gelation

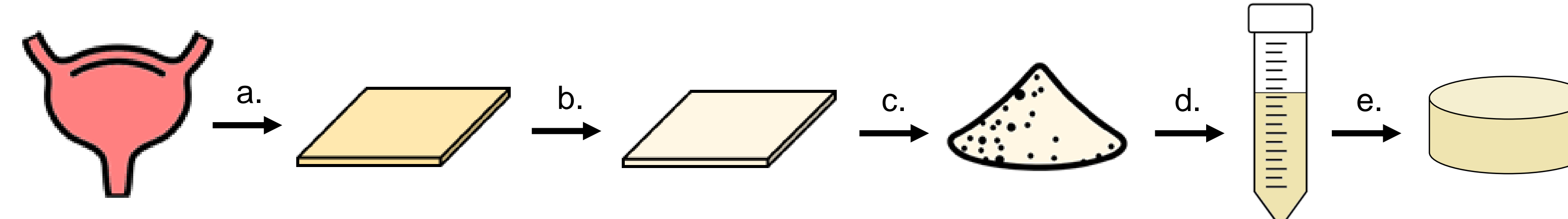


Fig. 1. Schematic representation of UBM hydrogel fabrication. (a) Whole porcine bladders were cleaned, distended overnight, and dissected to isolate UBM. (b) Native UBM was decellularized to yield an acellular biomaterial. (c) Decellularized UBM was frozen, lyophilized, and ground into a particulate form. (d) Decellularized, powdered UBM was then fully digested in a pepsin solution over 72 hrs. (e) The resultant digested UBM was neutralized and diluted before gelation in a cylindrical mold at 37° C.

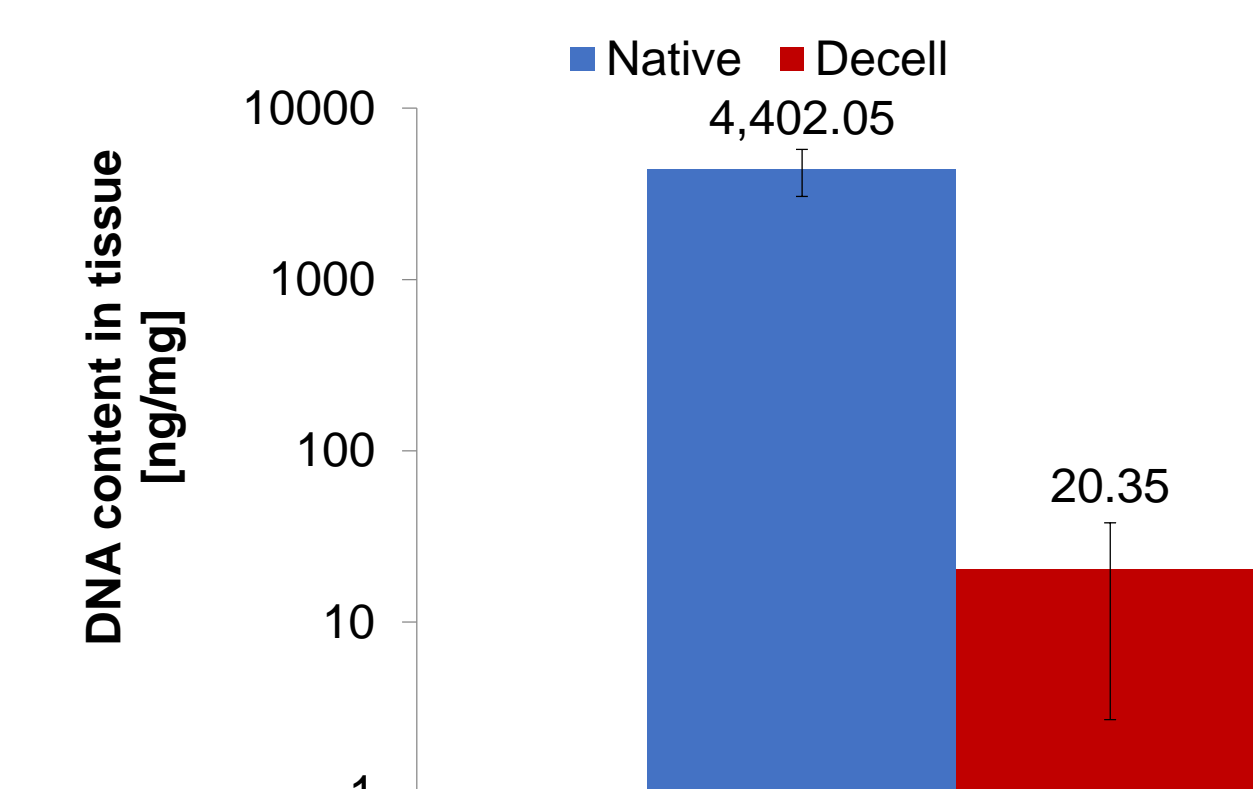


Fig. 2. DNA content of native and decellularized UBM. Two sample t-test was conducted for UBM DNA content before and after decellularization (n=3). Data is reported as mean ± standard deviation.

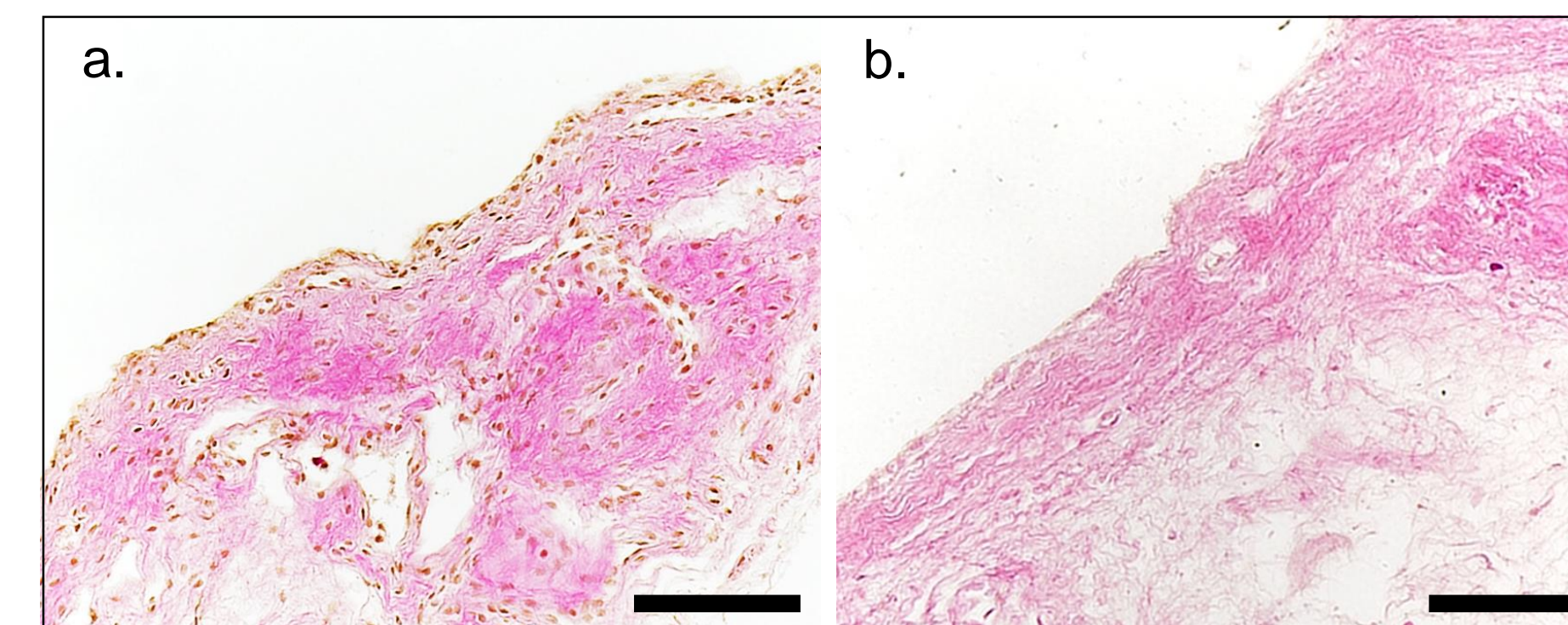


Fig. 3. H&E Staining of (a) native and (b) decellularized UBM sections. Brown coloring indicates cell nuclei, and pink indicates ECM tissue. Scale bar = 100 μm.

Following isolation and decellularization of porcine UBM (Fig. 1a,b), PicoGreen DNA content analysis showed that the overall DNA content was reduced from $4,402 \pm 1341$ ng DNA/mg dry tissue to 20.35 ± 17.66 ng DNA/mg dry tissue. This corresponds to a >99.5% reduction in native DNA content (Fig. 2). Decellularization was qualitatively observed in histological sections of UBM due to the absence of nuclear staining after decellularization (Fig. 3).

Gradient Hydrogel Development

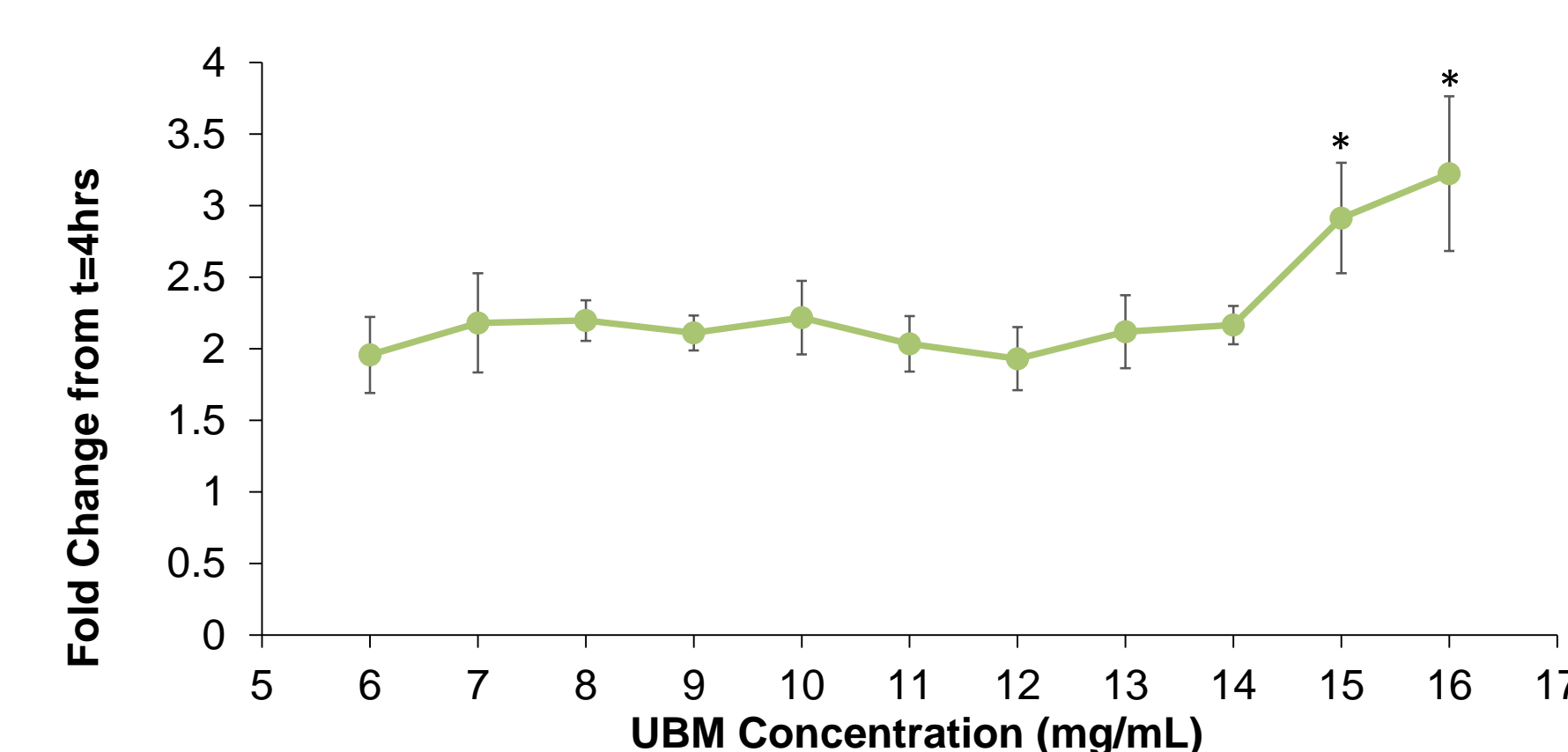


Fig. 4. L929 Fibroblast metabolic activity on UBM hydrogels after 72 hours. XTT absorbance fold change from t=4 hrs for varying UBM hydrogel substrate concentrations. One-way ANOVA (n=3, p<0.05). Data is reported as mean ± standard deviation.

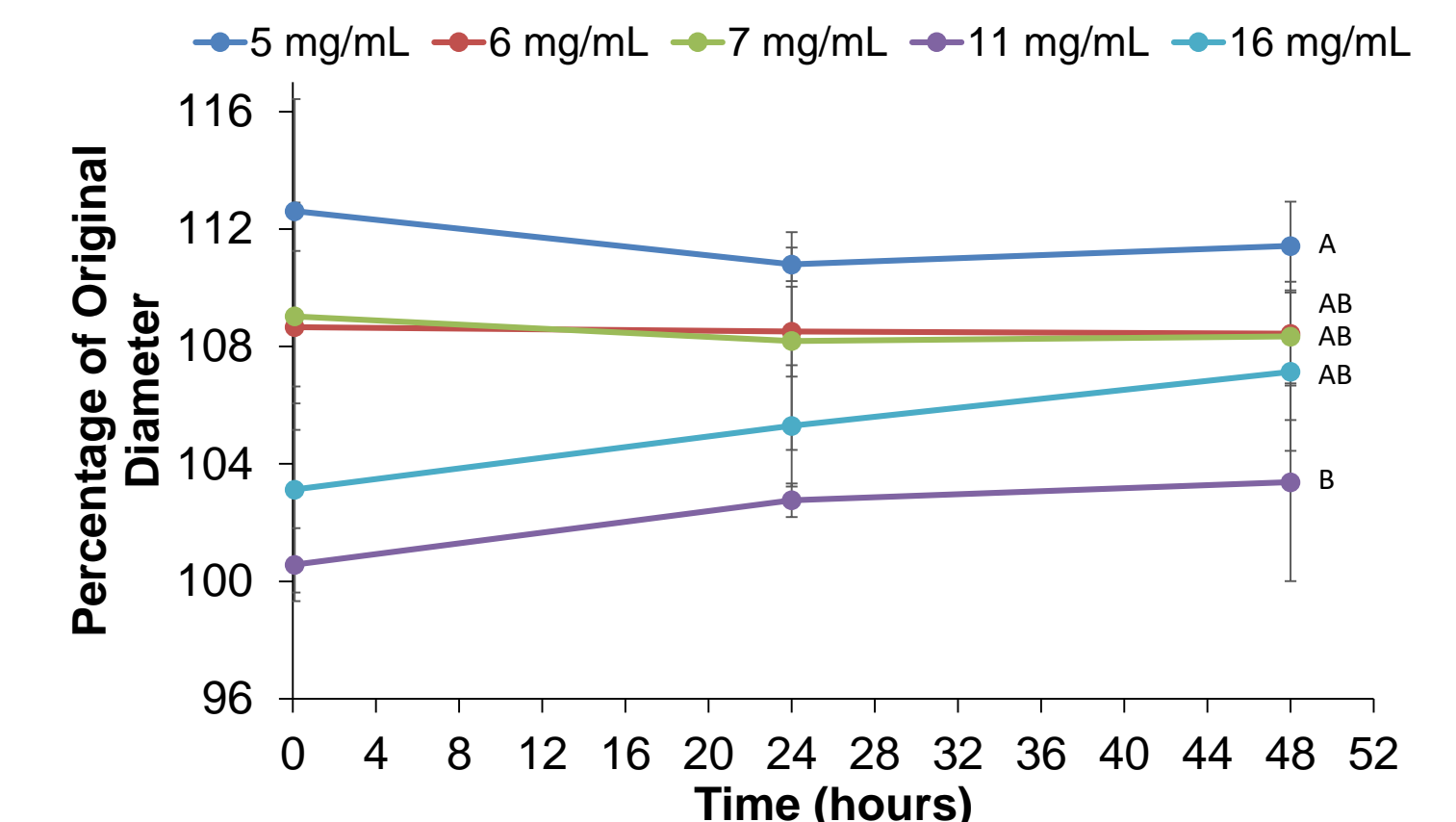


Fig. 5. Diameter change of UBM hydrogels. Percentage of original diameter after gelation over 48 hr incubation time in PBS. One-way ANOVA was conducted across all concentrations at t=48 hours (n=3). Data is reported as mean ± standard deviation.

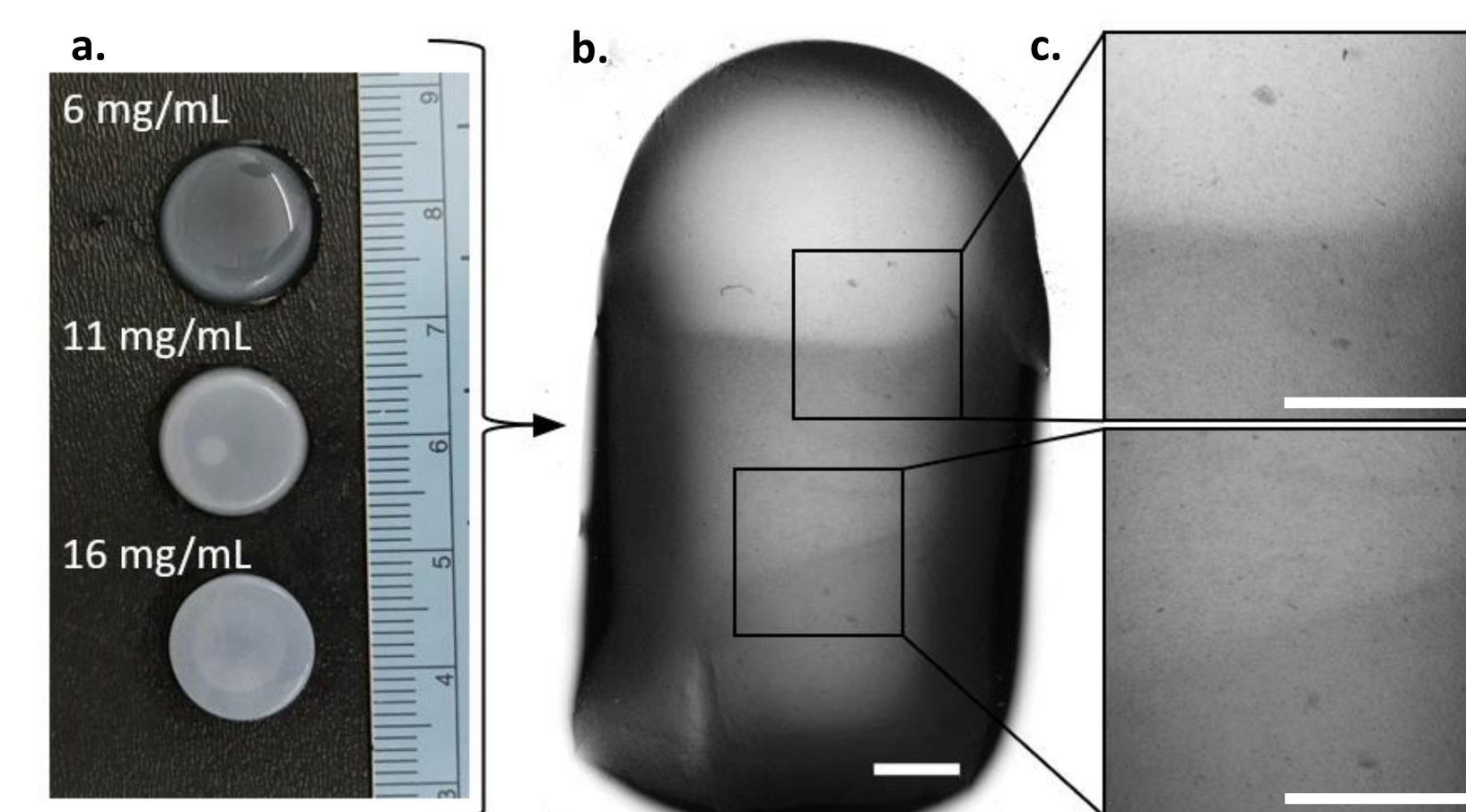


Fig. 6. Single-concentration UBM hydrogels and composite gradient hydrogel. (a) Macroscopic images of UBM hydrogels of 6, 11, and 16 mg/mL UBM concentration. (b) Brightfield cross-section of a hydrogel with an incorporated UBM density gradient. Scale bars = 1 mm. (c) Defined transition between regions of differing UBM density.

XTT analysis of cells seeded onto 15 and 16 mg/mL UBM hydrogels exhibited significantly greater metabolic activity than gels of 6-14 mg/mL UBM (Fig. 4), so 16 mg/mL was selected as the high-end UBM concentration for the gradient. The low-end UBM concentration selected was 6 mg/mL, as its diameter change over 48 hours in PBS was not significantly different than that of 16 mg/mL hydrogels (Fig. 5). Gradient gels were observed to have distinct regions of varying UBM concentrations (Fig. 6b,c), and the complex viscosity of gradient gels fell within the range of non-graded UBM gels, indicating integration of the three layers. (Fig. 7).

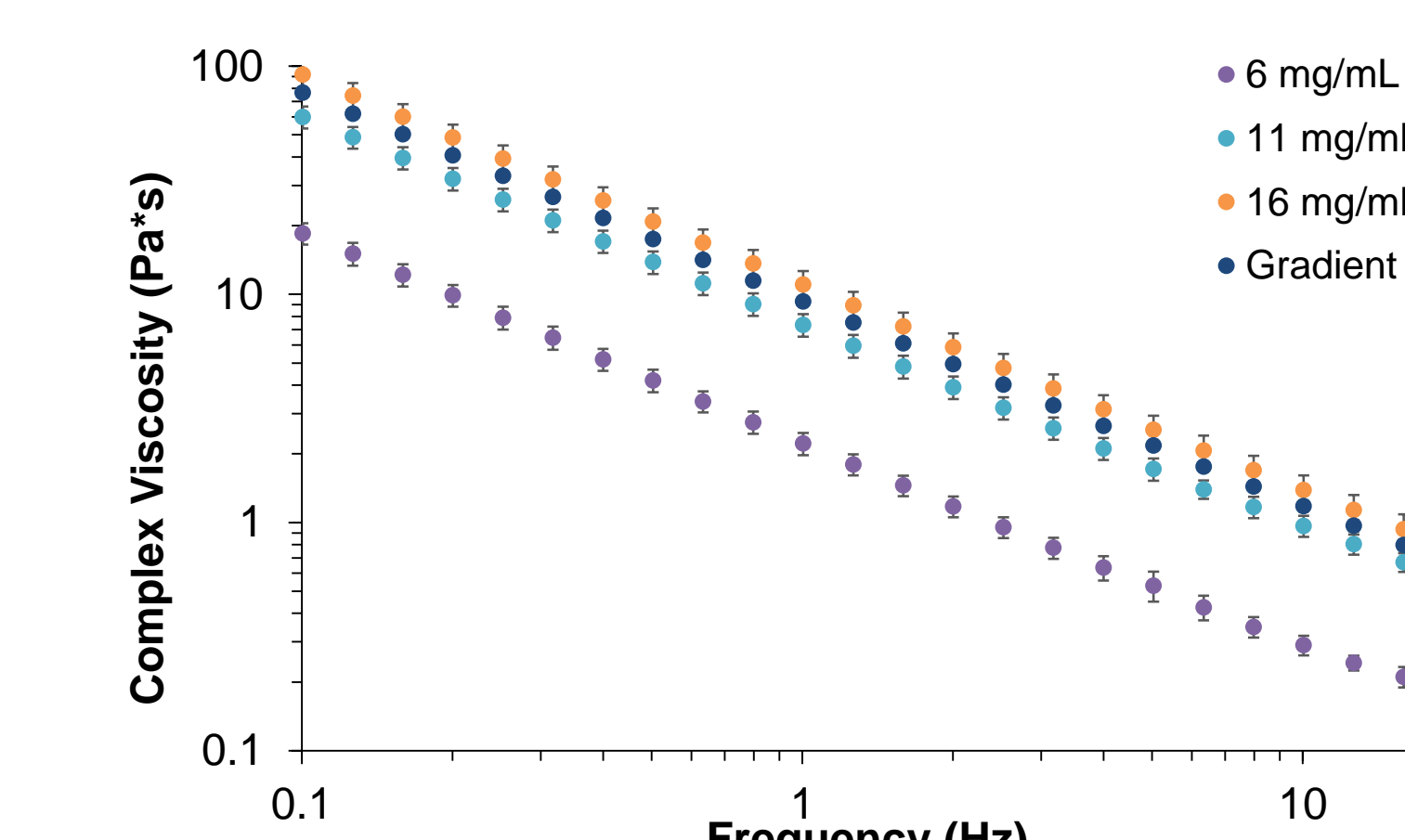


Fig. 7. Rheological characterization of UBM hydrogels. Complex viscosity $[\eta^*]$ for 6, 11, and 16 mg/mL and gradient UBM hydrogels over a range of frequencies (n=3). Data is reported as mean ± standard deviation.

Collagenase Degradation

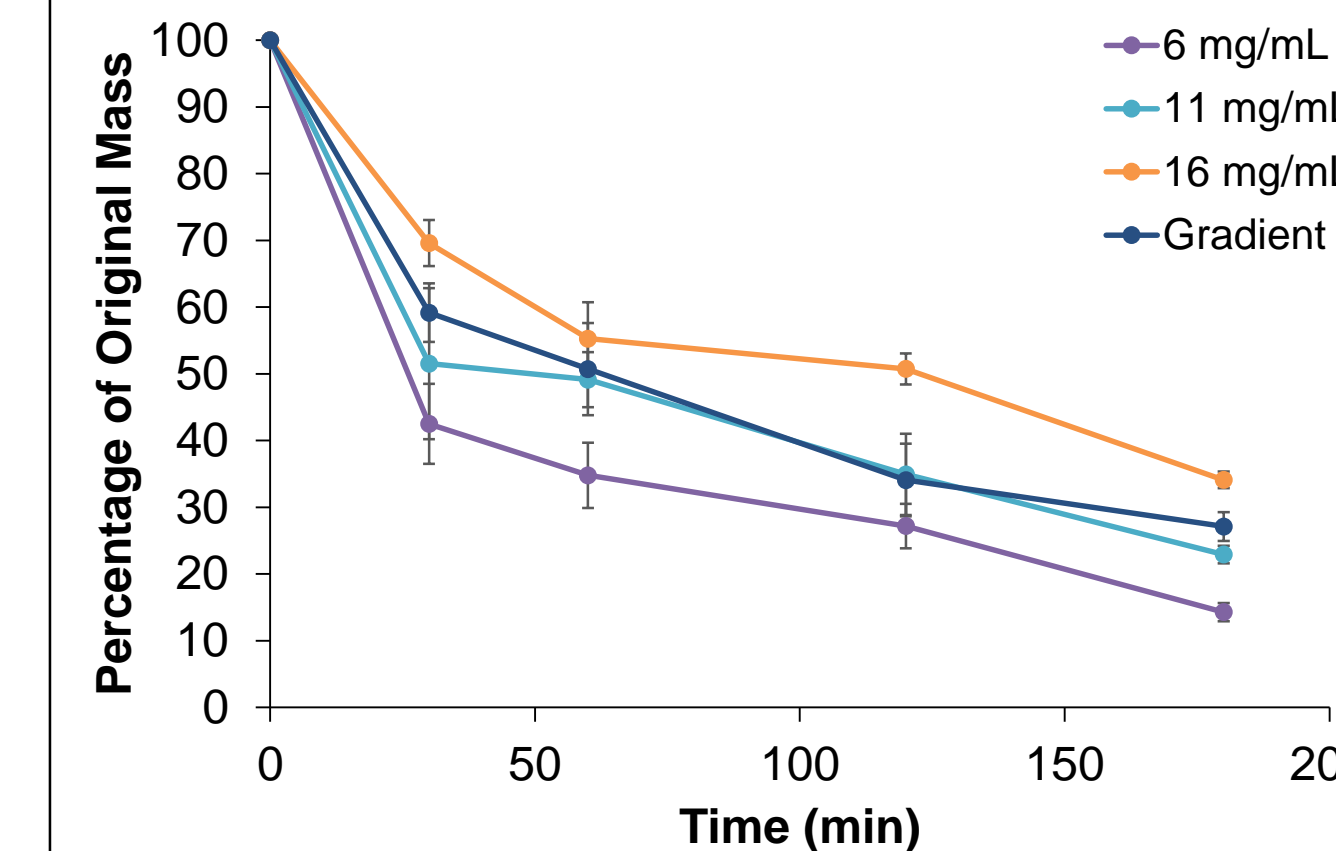


Fig. 8. Hydrogel Dry Mass Loss in Collagenase. Percentage of original dry mass over 3 hr incubation in collagenase I solution (n=3). Data is reported as mean ± standard deviation.

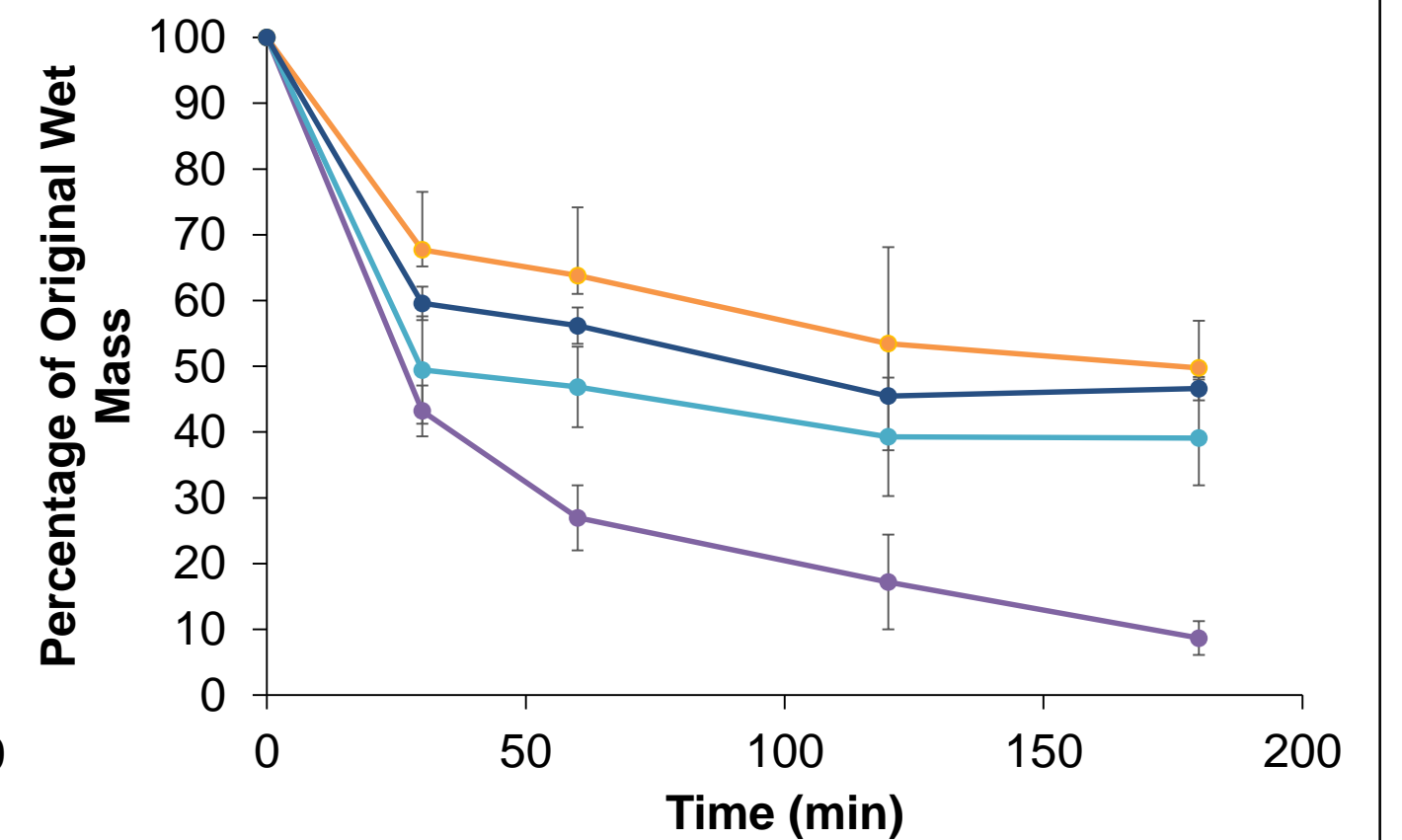


Fig. 9. Hydrogel Wet Mass Loss in Collagenase. Percentage of original hydrated mass over 3 hr incubation in collagenase I solution (n=3). Data is reported as mean ± standard deviation.

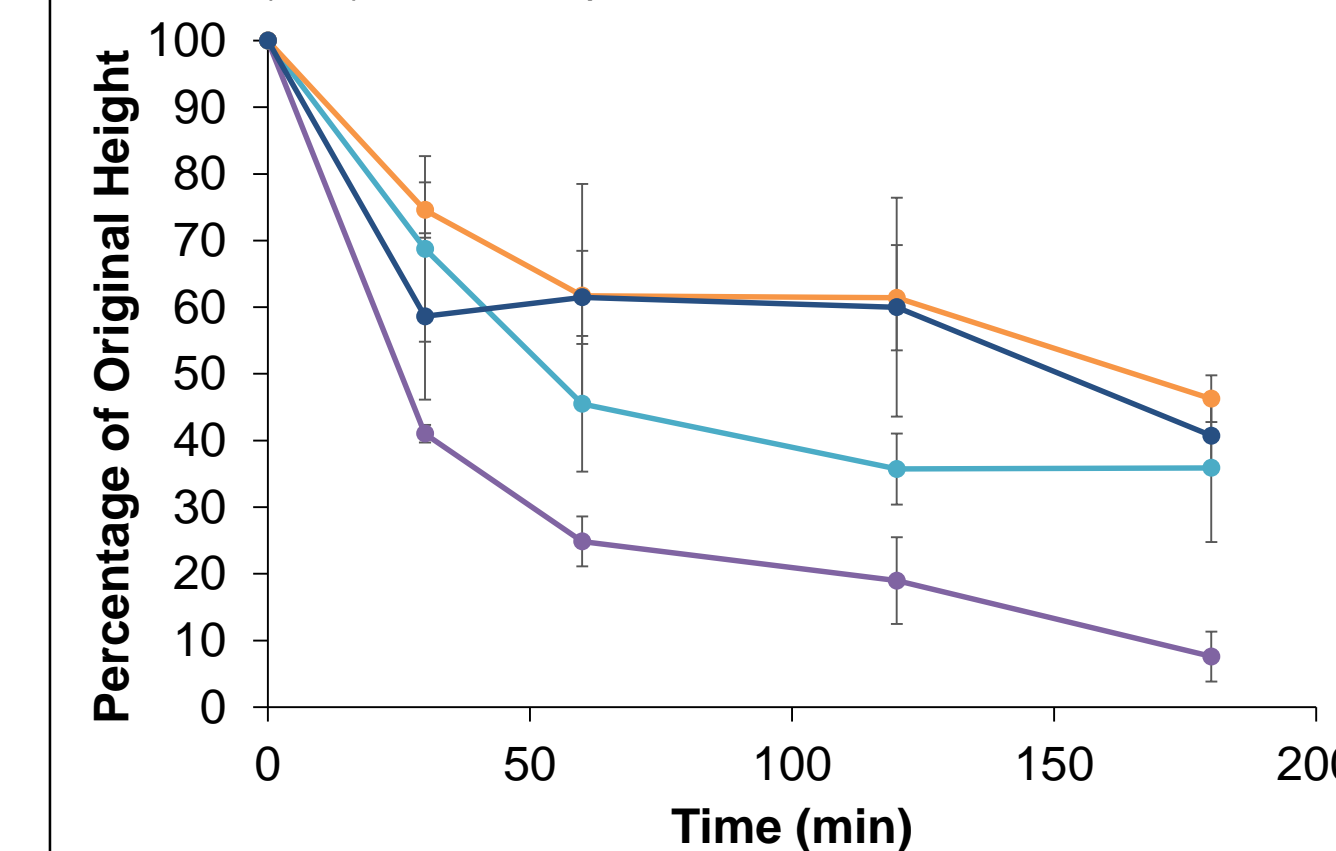


Fig. 10. Hydrogel Height Change in Collagenase. Percentage of original gel height over 3 hr incubation in collagenase I solution (n=3). Data is reported as mean ± standard deviation.

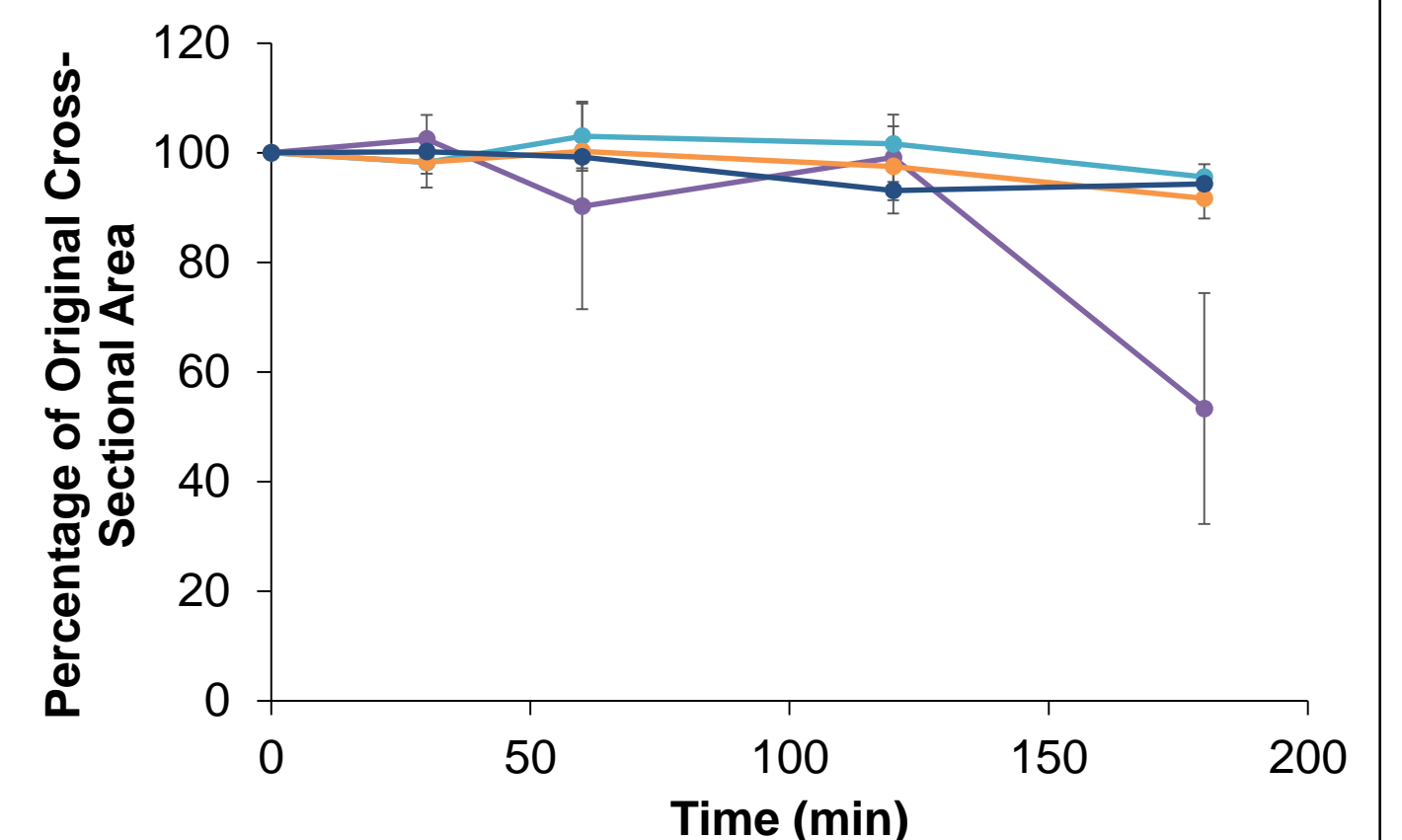


Fig. 11. Hydrogel Cross-Sectional Area Change in Collagenase. Percentage of original cross-sectional area over 3 hr incubation in collagenase I solution (n=3). Data is reported as mean ± standard deviation.

Hydrogels were digested in 100 μg/mL collagenase I solution to mimic gel degradation *in vivo*. While 6, 11, and 16 mg/mL and gradient hydrogels showed similar trends in mass and height reduction as they were degraded (Fig. 8, 9, 10), the surface area of 11 mg/mL, 16 mg/mL, and gradient hydrogels remained relatively constant over 3 hour digestion (Fig. 11).

Conclusions & Future Work

We have successfully decellularized porcine UBM in order to prevent immunogenic responses to this UBM-based hydrogel wound dressing. We have also developed a mechanically stable hydrogel that contains a gradient of decellularized UBM. Fibroblast metabolic activity was shown to increase with UBM density, indicating that this gradient has the potential to increase cell survival as fibroblasts infiltrate into the hydrogel during the wound healing process. Furthermore, gradient UBM hydrogels exhibit height and mass loss in the presence of collagenase while the cross-sectional surface area of the wound dressing remains more stable with time. This finding is promising for the hydrogel's overall ability to retain its shape over time while serving as a cellular scaffold in the wound bed.

Future studies will investigate gradient-induced cellular infiltration to assess the suitability of this graded hydrogel as a wound dressing. Functionalization of the UBM hydrogel with growth factors involved in wound healing, such as TGF-β1, will promote fibroblast recruitment and wound site fibrosis in order to accelerate wound healing and improve patient outcomes.

References & Acknowledgements

- (1) Frykberg, R. G., & Banks, J. (2015). Challenges in the Treatment of Chronic Wounds. *Advances in Wound Care*, 4(9), 560–582. doi: 10.1089/wound.2015.0635
- (2) Sen, C. K., Gordillo, G. M., Roy, S., Kirsner, R., Lambert, L., Hunt, T. K., ... Longaker, M. T. (2009). Human skin wounds: A major and snowballing threat to public health and the economy. *Wound Repair and Regeneration*, 17(6), 763–771. doi: 10.1111/j.1524-475x.2009.00543.x
- (3) Tschumperlin, D. J. (2013). Fibroblasts and the Ground They Walk On. *Physiology*, 28(6), 380–390. doi: 10.1152/physiol.00024.2013
- (4) Freytes, D. O., Martin, J., Velankar, S. S., Lee, A. S., & Badyal, S. F. (2008). Preparation and rheological characterization of a gel form of the porcine urinary bladder matrix. *Biomaterials*, 29(11), 1630–1637. doi:10.1016/j.biomaterials.2007.12.014
- (5) Gui, L., Chan, S. A., Breuer, C. K., & Niklason, L. E. (2010). Novel Utilization of Serum in Tissue Decellularization. *Tissue Engineering Part C: Methods*, 16(2), 173–184. doi:10.1089/ten.tec.2009.0120
- (6) Wolf, M. T., Daly, K. A., Brennan-Pierce, E. P., Johnson, S. A., Carruthers, C. A., Damore, A., ... Badyal, S. F. (2012). A hydrogel derived from decellularized dermal extracellular matrix. *Biomaterials*, 33(29), 7028–7038. doi: 10.1016/j.biomaterials.2012.06.051

This research was supported by the University of Maryland 2019 Summer Scholars Program and the NSF CBET (5246870)